Ultrasound in Med. & Biol., Vol. ■, No. ■, pp. 1–5, 2012

0301-5629/$ - see front matter

doi:10.1016/j.ultrasmedbio.2012.03.019

● *Technical Note*

RING ARRAY TRANSDUCERS FOR REAL-TIME 3-D IMAGING OF AN ATRIAL SEPTAL OCCLUDER

Edward D. Light, Brooks D. Lindsey, Joseph A. Upchurch, and Stephen W. Smith
Department of Biomedical Engineering, Duke University, Durham, NC, USA

(*Received* 22 *December* 2011; *revised* 19 *March* 2012; *in final form* 30 *March* 2012)

Abstract—We developed new miniature ring array transducers integrated into interventional device catheters such as used to deploy atrial septal occluders. Each ring array consisted of 55 elements operating near 5 MHz with interelement spacing of 0.20 mm. It was constructed on a flat piece of copper-clad polyimide and then wrapped around an 11 French O.D. catheter. We used a braided cabling technology from Tyco Electronics Corporation to connect the elements to the Volumetric Medical Imaging (VMI) real-time 3-D ultrasound scanner. Transducer performance yielded a –6 dB fractional bandwidth of 20% centered at 4.7 MHz without a matching layer vs. average bandwidth of 60% centered at 4.4 MHz with a matching layer. Real-time 3-D rendered images of an en face view of a Gore Helex septal occluder in a water tank showed a finer texture of the device surface from the ring array with the matching layer. (E-mail: ssmith@duke.edu) © 2012 World Federation for Ultrasound in Medicine & Biology.

Key Words: **2-D array transducer, Real-time 3-D imaging, Septal occluder.**

INTRODUCTION

Previously, we developed lead zirconate titanate (PZT)-based matrix array catheter transducers (Lee et al. 2004) and endoscopes (Pua 2004; Light et al. 2005) for real-time three-dimensional (3-D) ultrasound imaging. More recently, we have fabricated forward viewing ring array catheters for 3-D image guidance of interventional devices such as the vena cava filter and aortic aneurysm stent graft (Light et al. 2008) and trans-apical heart valves (Light et al. 2011). Other laboratories are developing side viewing 3-D catheters (Lee et al. 2011) and forward-viewing capacitive micromachined ultrasonic transducers (CMUT) ring arrays for electrophysiologic applications and real-time 3-D intravascular ultrasound (IVUS) (Degertekin et al. 2006; Yeh et al. 2006; Khuri-Yakub and Oralkan 2011).

Atrial septal defects (ASD) comprise up to 7% of total congenital heart lesions and as much as 25% of congenital heart disease in adults (Kaplan 1993). ASDs may go undetected for decades. If the ASD is small and the patient is asymptomatic, no action is taken. Otherwise, treatment options include open-heart surgery to repair the hole or catheter deployment of an atrial septal occluder. This minimally invasive procedure is often preferred by patients. The procedure is typically done under fluoroscopic guidance combined with transesophageal echo (TEE) and Doppler ultrasound (Ko et al. 2009) as well as two-dimensional (2-D) intracardiac echo (ICE) catheters (Hijazi et al. 2009) and even 3-D TEE (Perk et al. 2009). However, since the procedure already calls for the insertion of a catheter, we believe a catheter-based transducer capable of generating real-time 3-D images integrated into the occluder deployment kit might reduce the need for the other imaging modalities with the associated x-ray exposure of fluoroscopy and complexity and discomfort of TEE ultrasound. Real-time 3-D ultrasound enables continuous monitoring of cardiac structures and interventional devices before, during and after deployment. However, the integration of 3-D ultrasound imaging catheters into the deployment kits of interventional devices presents major challenges because of the requirement for dozens of active transducer channels to improve 3-D image quality and the severe fabrication difficulties in electrical connection to the submillimeter 2-D array elements. It is also important not to disrupt the original design of the device deployment kit. Figure 1 shows a schematic of an integrated ring array transducer, connected to the scanner *via* the system flex circuit and septal occluder deployment catheter. The

Address correspondence to: Stephen W. Smith, Department of Biomedical Engineering, Duke University, Rm 136 Hudson Hall, Durham, NC 27708. E-mail: ssmith@duke.edu

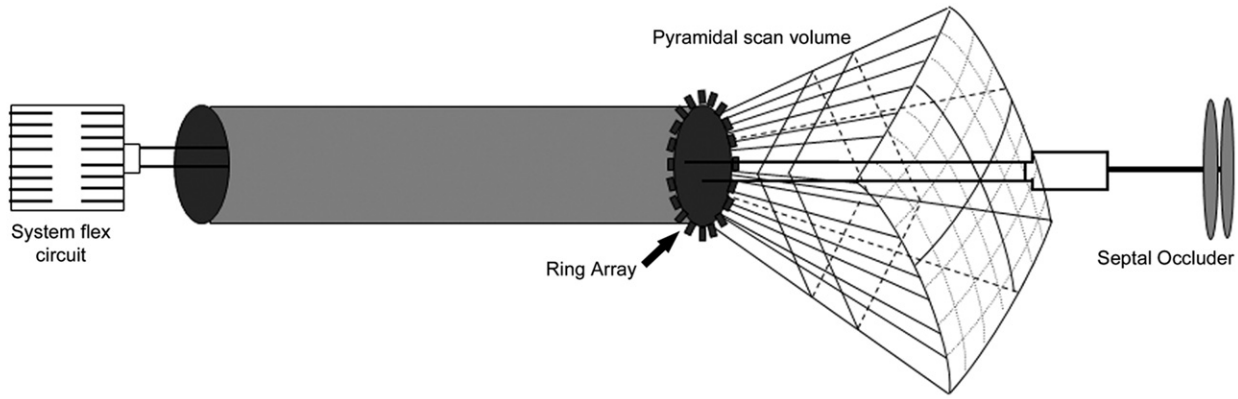

Fig. 1. Schematic of the integrated transducer and septal occluder deployment device. The real-time 3-D ultrasound pyramidal scan is directed outward from the distal end of the device and is co-axial with the deployment of the septal occluder.

real-time 3-D ultrasound pyramidal scan originates from the distal tip of the device, with the occluder exiting through the lumen. In this article, we describe the fabrication of such ring arrays operating near 5 MHz and the acquisition with a commercial scanner (Volumetrics Medical Imaging, Inc., Durham, NC, USA) of real-time 3-D ultrasound images of the Gore Helex septal occluder (W.L. Gore & Associates, Inc. Newark, DE, USA).

MATERIALS AND METHODS

We modified a commercial catheter deployment kit for our ring array transducers. This product uses an 8.5 Fr sheath (I.D.) resulting in an approximately 11 French (O.D.) catheter. This outer diameter determined the ring array diameter. We previously described ring array transducers using a small flexible circuit connected to our scanner system cable using Tyco Medical cabling (Tyco Electronics, Wilsonville, OR) (Light et al. 2009).

Figure 2 shows a schematic of the construction steps to build the ring array transducers. Construction begins with a metal-clad polyimide flexible circuit. This substrate has a shelf area where there is no metal (Fig. 2a). A beam of PZT ceramic (TRS Technologies, Inc., State College, PA, USA) was prepared that was 0.30 mm tall (thick), 0.18 mm wide and 11 mm long. In

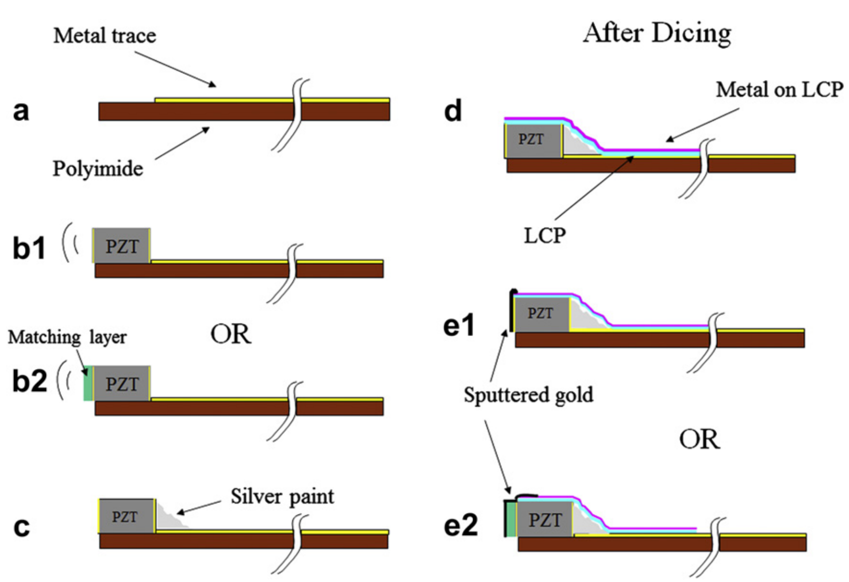

Fig. 2. A schematic of the steps to build the ring arrays. We start with a metallized polyimide substrate (a) having a metal-free shelf area to attach the PZT. We next attach the PZT beam/matching layer (2b1 and 2b2) with non-conductive epoxy. After the epoxy cures, silver paint is used to connect the back electrode of the PZT with the metal trace (c). The PZT is then diced, and wrapped around a catheter lumen. A 0.012 mm thick layer of liquid crystal polymer (LCP) is wrapped around the outer circumference of the PZT and polyimide substrate (d). This LCP layer is metallized with gold (shown in black) on one side only, the outer side, so that it does not risk shorting the traces together. A layer of gold is sputtered on the face of the elements and connected to the gold on the outside of the LCP (2e1 and 2e2).

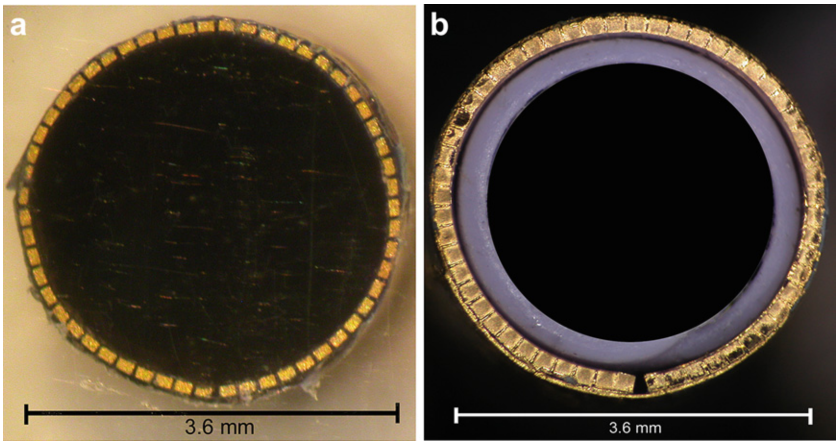

Fig. 3. Close up of ring arrays without matching layer (a) and with matching layer (b) after dicing and bonding to the liquid crystal polymer (LCP).

this work, we developed transducers with and without a single acoustic matching layer. The matching layer consists of a plate of the #107 matching layer from EBL Products, Inc. (East Hartford, CT, USA). Before attaching the PZT beam to our flex circuit, a .19 mm thick plate of the matching layer was metallized on both sides with 500 Å of nickel and 1000 Å of gold. The plate was then bonded to the PZT layer using a thin layer of Epotek 301 two-part epoxy (Billerica, MA, USA).

This beam/matching layer was attached to the polyimide with a low viscosity epoxy such that the beam was on its side (Fig. 2b1 and 2b2). With the beam on its side, the electroded portion of the PZT is pointed in the forward direction. After attaching the PZT, silver paint (SPI Supplies, West Chester, PA, USA) was applied such that it contacted the bottom electrode of the PZT and the flex circuit traces (Fig. 2c) on the polyimide. The transducer beam was then diced into 55 elements at a spacing of 0.2 mm and the entire device wrapped around a lumen with the same O.D. as the catheter lumen. A 0.012 mm thick layer of metallized liquid crystal polymer (LCP) was wrapped around the outer circumference of the PZT and polyimide substrate (Fig. 2d) and attached with epoxy (Hysol® E-60NC epoxy potting compound; (Loctite, Rocky Hill, CT)). The LCP keeps the transducer in a cylindrical shape. The Hysol epoxy fills the kerf so that there is an even surface on the front end of the transducer. We then sputter gold onto the face of the transducer and LCP. The transducer assembly was then attached to the clinical catheter and sent to Tyco Electronics Corporation for the cabling to be attached. After returning, a short piece of heat shrink (Advanced Polymers, Inc., Salem, NH, USA) was attached to seal the LCP and cover the wiring. For both transducers, the face of the elements was sealed with a thin layer of ultraviolet (UV) curing adhesive.

Figure 3 compares photographs of the 55-element ring arrays without matching layer (Fig. 3a) vs. with matching layer (Fig. 3b) after bonding to the LCP, but before cabling and adding the electrical grounding. Figure 3b includes the blue delivery catheter sheath. Figure 4 shows a close up of the cabling for the ring array transducer. The overall shield braid increases the lumen O.D. to 13 French.

We used standard 3-D phased array beaming forming techniques to generate our real-time 3-D images. Real-time 3-D ultrasound was developed in our laboratories at Duke University (Smith et al. 1991; von Ramm et al. 1991) and first commercialized for cardiovascular applications by Volumetrics Medical Imaging (VMI). The Duke/VMI 3-D system scans a 65°–120° pyramid with matrix array transducers of up to 500 active channels to produce 3-D scans at rates up to 30 volumes/s using 16:1 receive mode parallel processing. Real-time display options include up to five simultaneous image planes oriented at any desired angle, depth and thickness within the pyramidal scan as well as real-time 3-D volume rendering, 3-D pulse wave Doppler and 3-D color flow Doppler.

We scanned a 30 mm diameter Gore HX1530 Helex septal occluder (W.L. Gore & Associates, Inc.) in a water

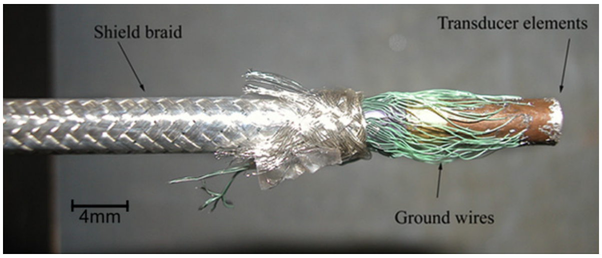

Fig. 4. Close up of the cabling for a 55-element ring array transducer. The signal wires are hidden by the green ground wires. The overall shield braid increases the lumen O.D. to 13 French. After wiring, the extra shield braid is cut back, and the exposed wires are sealed with 0.013 mm thick heat shrink.

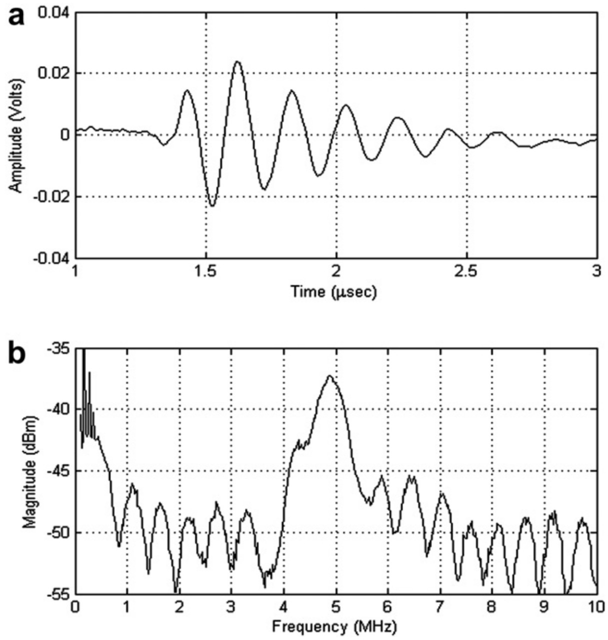

Fig. 5. Typical pulse echo response and spectrum of control array. The center frequency is 4.7 MHz and the –6 dB bandwidth is 20%.

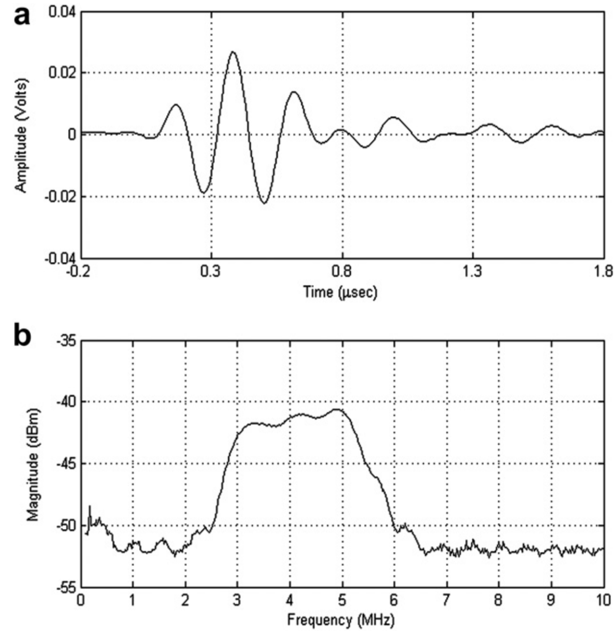

Fig. 6. Pulse echo response (a) and spectrum (b) from the transducer constructed with a single matching layer. The center frequency is 4.2 MHz and the –6 dB bandwidth is 68%.

tank. This device consists of a 10 Fr catheter delivery system and an implantable endoprosthesis comprised of a nickel-titanium (Nitinol) wire frame covered with expanded polytetrafluoroethylene (ePTFE). The ePTFE is treated with a proprietary coating to facilitate echocardiographic imaging of the occluder during implantation. When fully deployed, the occluder assumes a double disc configuration that bridges the septal defect to prevent shunting of blood between the right and left atria.

RESULTS

Figure 5 shows a typical pulse echo response (a) and power spectrum (b) of the control transducer without matching layer. For 12 elements mean center frequency is 4.7 MHz and the –6 dB bandwidth is 20%.

Figure 6 shows the pulse-echo response (a) and spectrum (b) of a single element from the ring array transducer with matching layer. For 12 elements mean center frequency is 4.28 MHz and the –6 dB bandwidth is 68%. The pulse echo sensitivity increased by 5% compared with the control array. Figure 7 shows a photograph of the W.L. Gore & Associates, Inc. HELEX septal occluder (a), a B-mode image plane from a real-time 3-D scan of the occluder (arrow) (b), a real-time 3-D rendered view of the occluder using the ring array without matching layer (c), and a real-time 3-D rendered view using the ring array with matching layer (d). The B-mode image shows the depth and thickness of the occluder. However, the figures show the immediate advantages of real-time 3-D imaging since the information content of the single B-mode image is minimal compared

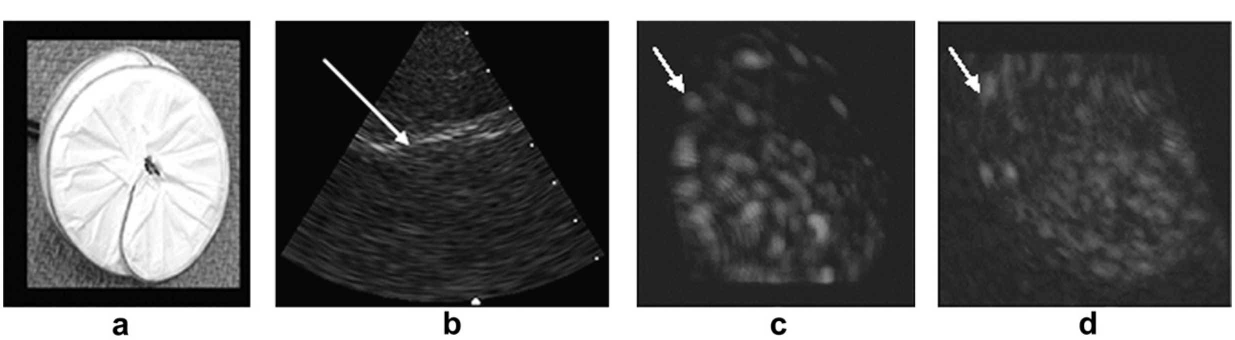

Fig. 7. Gore septal occluder photograph (a), B-mode plane with 1 cm scale marks (b), En face 3-D rendered view from control array (c) vs. matching layer array (d).

with the 3-D rendered views (c and d). The en face rendered images show the circular shape of the occluder, the nitinol ring as indicated by the arrows in Figure 7c and d, as well as the speckle pattern associated with the ePTFE fabric. A comparison of the rendered views also shows the finer speckle texture associated with the broader bandwidth of the matching layer array. Faint scan converter artifacts are also present.

DISCUSSION AND CONCLUSIONS

We developed new miniature ring array transducers integrated into interventional device catheters such as used to deploy atrial septal occluders. Such a catheter-based transducer capable of generating real-time 3-D images integrated with the occluder deployment kit might reduce the need for x-ray fluoroscopy and TEE ultrasound during the occluder deployment.

The ring arrays consisted of 55 elements operating near 5 MHz with interelement spacing of 0.20 mm. The development of matching layers and increased bandwidth for PZT ring arrays has been challenging. Boundary conditions for the transducer elements differ radically in each dimension since there is virtually no backing material, and each element is bonded to the flex circuit on one side and the catheter surface on the other side. Development of the matching layer, thus, proceeded by a trial and error process. Transducer performance yielded a –6 dB fractional bandwidth of 20% centered at 4.7 MHz without a matching layer vs. average bandwidth of 60% centered at 4.4 MHz with a matching layer. The 5% increase in pulse-echo sensitivity is modest and reflects the problem of anisotropic boundary conditions on the array elements.

Real-time 3-D rendered images of an en face view of a Gore Helex septal occluder (W.L. Gore & Associates, Inc.) in a water tank showed a finer texture of the device surface from the ring array with the matching layer. Previous studies have shown improved detection of speckle targets in tissue, such as the occluder surface, associated with the finer speckle texture linked to improved spatial resolution and higher bandwidth (Smith et al. 1983). However, image quality of the 3-D ring array catheters is still not acceptable. Image quality may be improved through the use of ring arrays of multiple rings to increase signal to noise ratio or synthetic aperture processing to reduce side lobe clutter associated with the ring geometry (Wang et al. 2002).

Acknowledgments—This research was supported by NIH grant HL089507.

REFERENCES

Degertekin FL, Guldiken RO, Karaman M. Annular-ring CMUT arrays for forward-looking IVUS: Transducer characterization and imaging. IEEE Trans Ultrason Ferroelectr Freq Control 2006;53: 474–482.

Hijazi ZM, Shivkumar K, Sahn DJ. Intracardiac echocardiography during interventional and electrophysiological cardiac catheterization. Circulation 2009;119:587–596.

Kaplan S. Congenital heart disease in adolescents and adults. Natural and postoperative history across age groups. Cardiol Clin 1993;11: 543–556.

Khuri-Yakub BT, Oralkan O. Capacitive micromachined ultrasonic transducers for medical imaging and therapy. J Micromech Microeng 2011;21:54004–54015.

Ko SF, Liang CD, Yip HK, Huang CC, Ng SH, Huang CF, Chen MC. Amplatzer septal occluder closure of atrial septal defect: Evaluation of transthoracic echocardiography, cardiac CT, and transesophageal echocardiography. AJR Am J Roentgenol 2009;193:1522–1529.

Lee W, Griffin W, Wildes D, Buckley D, Topka T, Chodakauskas T, Langer M, Calisti S, Bergstol S, Malacrida JP, Lanteri F, Maffre J, McDaniel B, Shivkumar K, Cummings J, Callans D, Silvestry F, Packer DA. 10-Fr ultrasound catheter with integrated micromotor for 4-D intracardiac echocardiography. IEEE Trans Ultrason Ferroelectr Freq Control 2011;58:1478–1491.

Lee W, Idriss SF, Wolf PD, Smith SW. A miniaturized catheter 2-D array for real-time, 3-D intracardiac echo cardiography. IEEE Trans Ultrason Ferroelectr Freq Control 2004;51:1334–1346.

Light ED, Angle JF, Smith SW. Real-time 3-D ultrasound guidance of interventional devices. IEEE Trans Ultrason Ferroelectr Freq Control 2008;55:2066–2078.

Light ED, Idriss SF, Sullivan KF, Wolf PD, Smith SW. Real-time 3-D ultrasonic laparoscopy. Ultrason Imaging 2005;27:89–100.

Light ED, Lieu V, Smith SW. New fabrication techniques for ring-array transducers for real-time 3-D intravascular ultrasound. Ultrason Imaging 2009;31:247–256.

Light ED, Lieu V, Smith SW. Progress in ring array transducers for real-time 3-D ultrasound guidance of cardiac interventional devices. Ultrason Imaging 2011;33:197–204.

Perk G, Lang RM, Garcia-Fernandez MA, Lodato J, Sugeng L, Lopez J, Knight BP, Messika-Zeitoun D, Shah S, Slater J, Brochet E, Varkey M, Hijazi Z, Marino N, Ruiz C, Kronzon I. Use of real-time three-dimensional transesophageal echocardiography in intracardiac catheter based interventions. J Am Soc Echocardiogr 2009; 22:865–882.

Pua EC, Idriss SF, Wolf PD, Smith SW. Real-time 3-D transesophageal echocardiography. Ultrason Imaging 2004;26:217–232.

Smith SW, Pavy HE, von Ramm OT. High speed ultrasound volumetric imaging system part I: Transducer design and beam steering. IEEE Trans Ultrason Ferroelectr Freq Control 1991;38:100–108.

Smith SW, Wagner RF, Sandrik JM, Lopez H. Low contrast detectability and contrast detail analysis in medical ultrasound. IEEE Trans Sonics Ultrason 1983;30:164–173.

von Ramm OT, Smith SW, Pavy HE. High speed ultrasound volumetric imaging system part II: Parallel processing and display. IEEE Trans Ultrason Ferroelectr Freq Control 1991;38:109–115.

Wang Y, Stephens DN, O'Donnell M. Optimizing the beam pattern of a forward-viewing ring-annular ultrasound array for intravascular imaging. IEEE Trans Ultrason Ferroelectr Freq Control 2002;49: 1652–1664.

Yeh DT, Oralkan O, Wygant IO, O'Donnell M, Khuri-Yakub BT. 3-D ultrasound imaging using a forward-looking CMUT ring array for intravascular/intracardiac applications. IEEE Trans Ultrason Ferroelectr Freq Control 2006;53:1202–1211.